Modeling of tritium transport and release in out-of-pile experiments

Alya A. Badawi, Anas M. Khaial and Mohamed E. Nagy
Nuclear Engineering Department, Alexandria University, Alexandria, Egypt

A model has been developed to describe the tritium transport behavior in lithium-containing ceramics in out-of-pile experiments. This model includes several transport mechanisms, such as tritium diffusion in the grains, adsorption and desorption at the grain surface, and diffusion through the network of interconnected pores. A computer code has also been developed, based on the model. The code was used to calculate the tritum release in CREATE III and OSI-E23 out-of-pile experiments. The model results were found to be in good agreement with the experiment.

تم تطوير نموذج لوصف عملية انتقال التريتيوم داخل المواد الخزفية المحتوية على الليثيوم في تجارب خارج الركامة. يحتوي النموذج على عدة آليات لانتقال التريتيوم، مثل عملية الإنتشار في يحبيبات المادة، والإدمصاص والمج من سطح الحبيبات، علاوة على الإنتشار خلال شبكة الفراغات الداخلية المتصلة ببعضها البعض. كما تم تطوير برنامج حاسب آلي يأخذ في الإعتبار كل العمليات السابق ذكرها. تم استخدام البرنامج لحساب انطلاق التريتيوم من المواد طبقا لما تم قياسة في تجربتين معمليتين خارج الركامة. أظهرت نتائج النموذج تطابقا مع نتائج التجارب.

Keywords: Fusion, Out-of-pile experiments, Blanket, Solid breeders, Tritium

1. Introduction

Interest in the use of solid lithium-based materials as tritium breeders for fusion blankets has grown since the late 1970s [1]. Solid breeders are currently being considered in Phase 3 in ITER [2,3]. Tritium behavior and transport in the blanket are particularly important in determining whether they will be used. The tritium behavior also determines the width of the operating temperature window for the solid breeder based on acceptable tritium inventory levels. A large inventory is undesirable from both a self-sufficiency as well as safety point of view [4].

Because of the importance of tritium transport in solid breeder blankets, several experiments have been done to evaluate the feasibility of utilization of various breeding materials in a fusion power plant and to determine the tritium retention and release characteristics of lithium ceramics as a function of different parameters such as temperature, microstructure, purge gas flow rate and chemical composition, generation rate and burnup [5]. Tritium recovery experiments have focused on the release process with the objective of characterizing the rate-limiting phenomena [6].

One type of experiments is the out-of-pile, where the sample is placed in a container and irradiated while the container is sealed. The container is then opened and the released tritium is measured. The results of the out-of-pile experiments are accurate, due to the closeness between the samples and the measuring device, which decreases the losses due to leakage and adsorption.

In order to successfully model tritium release in ceramic breeders, it is necessary to have a precise physical understanding of the relevant mechanisms involved. Such an understanding has been sought for many years, but is yet to be achieved, due to experimental difficulties and the very complicated nature of the processes involved.

To generate confidence in the results provided by models and to assess their predictive capabilities, it is necessary to compare computed results with experimental data. In this respect, calibration analysis must be carried out in parallel with model development and aim at defining the confidence level of the predictions for the ranges of parameters and operating conditions to which the model can

be applied and to assess the influence of key variables affecting the overall kinetics of the release.

A model has been developed to describe the tritium transport behavior in out-of-pile experiments. This model includes several transport mechanisms, such as tritium diffusion through in the grains, adsorption and desorption at the grain surface, and diffusion through the network of interconnected pores. A computer code has also been developed, based on the model. This code can be used to calculate the tritium release in out-of-pile experiments.

2. Model description

The developed model divides the material into a number of unit cells. Fig. 1 shows a schematic diagram of the model unit cell which contains a number of grains, surface, and pore. The grain boundary diffusion in the present model is bypassed. This was adopted in the subsequent analysis due to lack of data on the tritium diffusion coefficient and the dimensions of the grain boundaries.

The number of grains, N_g, in a unit cell is calculated from [7]:

$$N_g = \frac{(1-\varepsilon)}{\varepsilon}\frac{\pi r_{ip}^2 L_e}{v_g}, \quad (1)$$

where; ε is the porosity, r_{ip} is the pore radius and v_g is the grain volume. L_e is the effective pore length, calculated from [8]:

$$L_e = \frac{L}{\sqrt{\varepsilon}}, \quad (2)$$

where L is the pore length.

There are two types of hydrogen isotopes inside the unit cell: the tritium (T or ^{3}H) present due to the lithium irradiation, and the hydrogen (H or ^{1}H) present due to diffusion from the purge gas, which usually contains a small amount of hydrogen.

The equation describing the diffusion inside the grain is [7]:

$$\frac{\partial Cg(r,t)}{\partial t} = D_g(T)\left(\frac{\partial^2 Cg(r,t)}{\partial r^2} + \frac{2}{r}\frac{\partial Cg(r,t)}{\partial r}\right). \quad (3)$$

Where $C_g(r,t)$ is the tritium/hydrogen concentration in the grain at position r and time t (at/m^3), $D_g(T)$ is the tritium/hydrogen diffusion coefficient in the grain as a function of temperature T (m^2/s). Note that there is no term to account for tritium generation in eq. (3). This is because in out-of-pile experiments the tritium is extracted from the sample after, and not during, irradiation, and hence generation.

The boundary conditions used to solve the above equation are:

1- Symmetry at $r = 0$

$$\left(\frac{\partial Cg(r,t)}{\partial r}\right)_{r=0} = 0. \quad (4)$$

2- Convection at $r = r_g$

$$-D_g(t)\left(\frac{\partial Cg(r,t)}{\partial r}\right)_{r=rg} = (\Re_\beta - \Re_{diss})A_{s/g}. \quad (5)$$

Where $\Re_\beta$ is the flux of atoms going to the surface from the grain (at/m^2 s) and $\Re_{diss}$ is the flux of atoms going to the grain from the surface (at/m^2 s). $A_{s/g}$ is the surface area per unit grain area.

There are four types of surface fluxes coming in and out of the surface, as shown in fig. 2. Those fluxes are:

1. A flux of atoms (tritium or hydrogen) entering the surface from the bulk side [9]:

$$\Re_\beta = k_\beta Cg(r_g,t)\,(1-\theta), \quad (6)$$

$$k_\beta(T) = \beta_o \exp(-E_\beta / RT). \quad (7)$$

$k_b(T)$ and β_o are in (m/s). β_o can be estimated based on the vibration frequency of the atoms [10]:

$$\beta_o = \frac{10^{13}}{\sqrt{N_s}}, \quad (8)$$

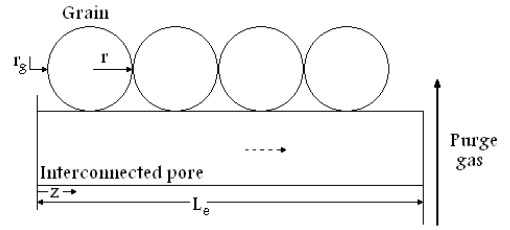

Fig. 1. Schematic diagram of the model unit cell.

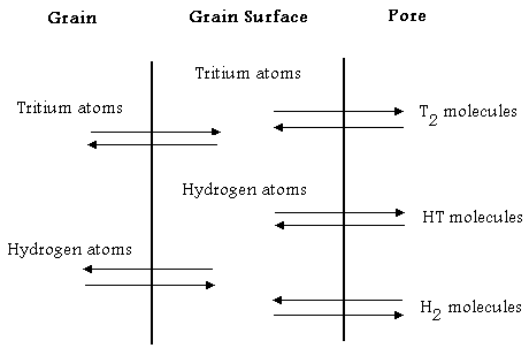

Fig. 2. Schematic diagram showing the different hydrogen species and fluxes in the model.

where θ is the total surface coverage, defined as the fraction of surface sites filled with T- or H-atoms, E_β is the activation energy for adsorption from the grain (J/mol), N_s is the number of surface sites *(sites/*m^2*)*, and R is the universal gas constant (J/mol K).

2. A flux of molecules of species (i) (tritium or hydrogen-containing molecule) entering the surface from the pore side[9]:

$$\Re_{ads}^{(i)} = k_{ads}^{(i)}(T,\theta)\, Cp^{(i)}(z,t)\,(1-\theta)^2\,, \qquad (9)$$

and $k_{ads}^{(i)}(T,\theta)$ *(m/*s*)* is calculated from [11],

$$k_{ads}^{(i)}(T,\theta) = \frac{\sigma\, z_{adj}}{\sqrt{8\times10^{-3}\pi}}\sqrt{\frac{RT}{M^{(i)}}}\,exp(-2E_{ads}(\theta)/RT)\,. \qquad (10)$$

where; $C_p^{(i)}(z,t)$ is the concentration of gaseous species (i) in the pore at position z and time t (molec/m^3), $E_{ads}(\theta)$ is the activation energy of adsorption (J/mol), σ is the condensation or trapping coefficient, z_{adj} is the number of adjacent sites, and, M_i is the molecular weight of species (i) (kg/kmol).

3. A flux of molecules of species (i) leaving the surface to the pore (the desorption flux) [9]:

$$\Re_{des}^{(i)} = k_{des}(T,\theta)\,\theta^j\theta^k\,, \qquad (11)$$

$$k_{des}(T,\theta) = \frac{1}{2}\frac{N_s z_{adj} RT}{N_A h}\,exp(-2E_{des}(\theta)/RT)\,, \qquad (12)$$

where; $E_{des}(\theta)$ is the activation energy of desorption (J/mol), N_A is Avogadro's number (part/mol), h is Planck's constant (J s), θ^k and θ^j are the surface coverages of atomic species k and j, respectively, that constitute the molecule (i). The factor 2 in the exponential is due to the fact that two atoms desorb to form one molecule.

4. A flux of atoms leaving the surface to the grain [5]:

$$\Re_{diss} = k_{diss}(T)\theta\,, \qquad (13)$$

$$k_{diss}(T,\theta) = \frac{N_s z_{adj} RT}{N_A h}\,exp(-E_{diss}(\theta)/RT)\,. \qquad (14)$$

where E_{diss} is the activation energy of dissolution (J/mol).

The surface coverage of tritium, θ_T, is obtained by solving the coverage rate equation:

$$\frac{d(N_s\theta_T)}{dt} = \Re_\beta^T - \Re_{diss}^T + 2\Re_{ads}^{T_2} + \Re_{ads}^{HT} - 2\Re_{des}^{T_2} - \Re_{des}^{HT}. \qquad (15)$$

Similarly, for hydrogen:

$$\frac{d(N_s\theta_H)}{dt} = \Re_\beta^H - \Re_{diss}^H + 2\Re_{ads}^{H_2} + \Re_{ads}^{HT} - 2\Re_{des}^{H_2} - \Re_{des}^{HT}. \qquad (16)$$

The total surface inventory, θ, is equal to the summation of the surface coverages of the hydrogen and tritium, i.e.:

$$\theta = \theta_T + \theta_H\,. \qquad (17)$$

The activation energies of the four fluxes are related through the activation energy of

solution, E_s, as well as the heat of adsorption, Q [12]:

$$E_s = (E_{diss} - E_\beta) - (E_{des} - E_{ads}), \quad (18)$$

$$Q = E_{des} - E_{ads}. \quad (19)$$

The pore is modeled as a straight cylinder of length L_e. Pore diffusion is assumed to be one-dimensional. For gas species (i) [7]:

$$\frac{\partial Cp^{(i)}(z,t)}{\partial t} = \frac{\partial}{\partial z}\left(D_{peff}^{(i)} \frac{\partial Cp^{(i)}(z,t)}{\partial z} \right) + (\Re_{des}^{(i)} - \Re_{ads}^{(i)}) \times \frac{2}{r_{ip}}. \quad (20)$$

where; $D_{peff}^{(i)}$ is the effective pore diffusion coefficient for species (i) (m^2/s). The factor ($2/r_{ip}$) is the ratio between the peripheral area-to-volume of the pore (m^{-1}) [5].

There are three regimes possible for the calculation of $D_{peff}(T)$, depending on the pressure, temperature and mass of the diffusion atoms. These regimes are [7]:

1. Ordinary diffusion in which molecular collisions dominate the diffusion process.
2. Knudsen diffusion in which collisions of the diffusing molecules with the porous solid dominate the diffusion process.
3. A transition region between ordinary and Knudsen diffusion.

Estimation of the applicable regime depends on the ratio of the mean-free-path of the diffusing species, λ, to the characteristic pore radius, r_{ip}.

The boundary conditions used for solving the pore diffusion equation are [7]:

1. Zero concentration gradient for each species (i) at the beginning of the interconnected pore:

$$\left[\frac{\partial Cp^{(i)}(z,t)}{\partial z} \right]_{z=0} = 0. \quad (21)$$

2. Given concentration for each species (i) at the end of the interconnected pore system:

$$Cp^{(i)}(L_e,t) = C_{purge}^{(i)}. \quad (22)$$

The concentrations of different species in the pore can be calculated with the aid of the following equations [7]:

$$N_{HT} + 2N_{H_2} = N_H, \quad (23)$$

$$N_{HT} + 2N_{T_2} = N_T, \quad (24)$$

$$\frac{[N_{HT}]^2}{N_{T_2} N_{H_2}} = K, \quad (25)$$

where; N_{H2} is the number of H_2 molecules in the pore, N_{T2} is the number of T_2 molecules in the pore, N_{HT} is the number of HT molecules in the pore, N_H is the total number of hydrogen atoms in the pore, N_T is the total number of tritium atoms in the pore, and K is the equilibrium constant, which is estimated from tabulated values for different temperatures given by Jones [13].

3. Numerical approximations and solution techniques used in the code

The system of diffusion equations in the different regions of the model is solved by using a forward difference approximation for the time derivative and a control volume scheme for the spatial derivatives in both the grain and the pore. Each grain is divided into (nr) nodes, while the pore is divided into (nz) nodes. Therefore:

$$\Delta r = \frac{r_g}{nr - 1}, \text{ and} \quad (26)$$

$$\Delta z = \frac{L_e}{nz}. \quad (27)$$

Applying mass balance with forward time derivative results in the following equations.

a. The grain

$$Cg_k^{p+1} = Cg_k^p + \frac{D_g(T)\Delta t}{(\Delta r)^2}\left((\frac{r_{k-1}}{r_{k-1/2}})^2 Cg_{k-1}^p + (\frac{r_k}{r_{k-1/2}})^2 Cg_{k+1}^p - [(\frac{r_{k-1}}{r_{k-1/2}})^2 + (\frac{r_k}{r_{k-1/2}})^2] Cg_k^p \right), \quad (28)$$

Where the subscript, k, represents node position in the grain, and the superscript, p, represents the time step.

The boundary condition nodes are:

$$Cg_1^{p+1} = Cg_1^p + 3\frac{D_g(T)\Delta t}{(\Delta r)^2}(Cg_2^p - Cg_1^p), \quad (29)$$

and

$$Cg_{nr}^{p+1} = Cg_{nr}^p + \frac{D_g(T)\Delta t}{(\Delta r)^2}\left(\frac{r_{nr-1}}{r_{nr-1/2}}\right)^2 (Cg_{nr-1}^p - Cg_{nr}^p)\frac{\Delta t}{\Delta r}(\Re_{diss} - \Re_\beta)A_{s/g}, \quad (30)$$

b. The surface

The surface coverage of tritium and hydrogen at time step (p+1) is calculated from:

$$\theta_T^{p+1} = \theta_T^p + \frac{\Delta t}{N_s}\left(\Re_\beta^T - \Re_{diss}^T + 2\Re_{ads}^{T_2} + \Re_{ads}^{HT} - 2\Re_{des}^{T_2} - \Re_{des}^{HT}\right)^p, \quad (31)$$

$$\theta_H^{p+1} = \theta_H^p + \frac{\Delta t}{N_s}\left(\Re_\beta^H - \Re_{diss}^H + 2\Re_{ads}^{H_2} + \Re_{ads}^{HT} - 2\Re_{des}^{H_2} - \Re_{des}^{HT}\right)^p. \quad (32)$$

c. The pore

$$Cp_m^{p+1} = Cp_m^p + \frac{D_p(T)\Delta t}{(\Delta z)^2}(Cp_{m-1}^p + Cp_{m+1}^p - 2Cp_m^p) + \frac{2\Delta t}{r_{ip}}(\Re_{des}^{(i)} - \Re_{ads}^{(i)})^p. \quad (33)$$

The subscript, m, represents the node position in the pore. The boundary conditions in the pore become:

$$Cp_1^{p+1} = Cp_1^p + \frac{D_p(T)\Delta t}{(\Delta z)^2}\left(Cp_2^p - Cp_1^p\right) + \frac{2\Delta t}{r_{ip}}(\Re_{des}^{(i)} - \Re_{ads}^{(i)})^p, \quad (34)$$

and

$$Cp_{nz}^{p+1} = Cp_{nz}^p + \frac{D_p(T)\Delta t}{(\Delta z)^2}(Cp_{nz-1}^p + 2C_{purge} - 3Cp_{nz}^p) + \frac{2\Delta t}{r_{ip}}(\Re_{des}^{(i)} - \Re_{ads}^{(i)})^p. \quad (35)$$

The time increment, Δt, is chosen to be small enough to avoid the stiffness of the coverage equation, this small Δt satisfies the maximum constraint for stability conditions, which is found at the grain surface [14]:

$$3\frac{D_p\Delta t}{(\Delta z)^2} + \frac{2\Delta t}{r_{ip}}k_{ads}(1-\theta)^2 \le 1, \quad (36)$$

which corresponds to the last pore node (z=L_e).

The tritium release rate, RR, is computed from:

$$RR = N_p(37)\pi r_{ip}^2 \times \frac{\Delta z}{2} \times \sum_i n_i D_{peff}^{(i)} Cp_{nz}^{(i)}, \quad (37)$$

where the summation is carried over all tritium-containing species.

4. Model results and comparison with experimental data

Comparison between the results of the model and the experimental data is necessary in order to validate the developed model and show that it can produce reliable results. The experiments chosen to perform this comparison were the CREATE III [15] and OSI-E23 [16] experiments. Both experiments selected for model validation used $LiAlO_2$, which is considered to be the most promising solid breeder material [2].

In the CREATE III experiment, $LiAlO_2$ samples weighing from 50-100 mg were irradiated in NRX reactor for 48 h, flux averaging 7×10^{12} n/cm^2 s. The temperature was estimated to be <370K. He-1% H_2 sweep gas was used at flow rate of 0.5 l/min. All extraction tests were performed at 873K for 4 hr.

The total tritium recovered, which includes the free tritium, tritium released during the anneal and the residual tritium in the ceramic, ranged from 0.37 to 1.11 GBq per gram for samples with natural ^{6}Li enrichment, and from 7.4 to 16.6 GBq per gram for samples

with high ^{6}Li enrichment. The amount of residual tritium was generally less than 1% of the total [15].

In the OSI-E23 experiment, short irradiations in OSIRIS reactor of 3 to 5 mm spheres of lithium aluminate have been performed. Under a thermal flux of 1.3 to 2×10^{12} n/cm^2 s the tritium produced in the sphere was 3.7 to 4.5×10^6 Bq, depending on the sample weight (≤100 mg).

The sample container (quartz) was opened under a gas flow a few weeks after irradiations, enabling measurements at room temperature. The sphere is then allowed to fall in the furnace (generally preheated at a constant temperature), and the tritium released is measured.

More than 30 experiments were run in pure argon or in argon plus 0.1% hydrogen at a flow rate of 0.5 ml/s [16].

Table 1 includes the input data used in the computer code to calculate the tritium release from both experiments.

The heat of adsorption, Q, was obtained from Fischer data, in which Q changes with the total surface coverage [12]. The activation energy of adsorption, E_{ads}, was chosen to be 25 kJ/mol, which is between 15-50 kJ/mol, the range suggested by Badawi and Raffray [4]. However, a few code runs with different values of E_{ads} produced no effective change in the results. The value of the activation energy of desorption, E_{des}, was obtained from the relation in eq. (19) i.e.,

$$E_{des} = E_{ads} + Q. \tag{38}$$

The activation energy of solution, E_S, was chosen to be 40 kJ/mol, which is an average value between the activation energies of 25 kJ/mol for Li_2O [17,18] and 55 kJ/mol for Al_2O_3 [19], which are the two materials used to produce the $LiAlO_2$ [15, 16].

The number of nodes in the grain, surface and pore is chosen arbitrarily. However, increasing the number of nodes did not have an effect on the results.

Fig. 3 shows a comparison between the calculated and measured fractions of tritium released (the total tritium release/ the total tritium generated) for a period of 10 min in the CREATE III experiment. The figure shows that there is a good agreement between the experimental results and the model results. There is a difference of 13% between the calculated release and the measured release at about 2 min, and of 6% at about 3.5 min.

Fig. 4 shows a comparison between the calculated and measured fractional tritium release rates for a period of 1 hr. The figure shows that there is a shift of about 3 min between the calculated and the measured peaks of the tritium released from the sample. The calculations predicted a faster HT release than the actual case. The main reason for this error is that the model does not account for the oxygen present in the sample. The presence of oxygen in the pore, and hence of HTO and T_2O will slow the pore diffusion, which is a function of the mass of the diffusing species [7]. Slow pore diffusion will cause a slow tritium release form the pore and thus will shift the peak towards that measured in the experiment. However, accounting for the presence of the oxygen in the model is not feasible at this point because there is no data available on: (1) the activation energies for oxygen surface reactions, (2) the activation energies for OT and OH surface reactions, and (3) the number of surface sites available for oxygen in a sample.

The value of the maximum fractional release rate produced by the model was found to be <5% different from that produced by the experiment (see fig. 4).

5. Summary and conclusions

A model has been developed to describe the tritium transport behavior in lithium containing ceramics. This model includes several transport mechanisms, such as tritium diffusion in the grains, adsorption and

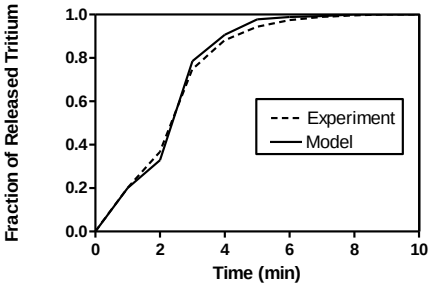

Fig. 3. Comparison between calculated and measured tritium release (CREATE III).

Table 1
Input data from CREATE III and OSI-E23 experiments

Material	CREATE III $LiAlO_2$	OSI-E23 $LiAlO_2$
Weight (kg)	0.1×10^{-3} [14]	0.1×10^{-3} [15]
Theoretical density (kg/m^3)	2610 [6]	2610 [6]
Porosity (%)	36 [14]	25 [15]
Grain radius (m)	0.4×10^{-6} [14]	0.14×10^{-6} [15]
Pore diameter (m)	1.29×10^{-6} [14]	1.3×10^{-6} *
Purge gas composition	He + 1% H_2 [14]	Ar + 1% H_2 [15]
Purge gas pressure (atm)	1.0 [14]	1.0 [15]
Grain diffusion coefficient:		2×10^{-9} [16]
Preexponential (m^2/s), D_o	2×10^{-9} [16]	90.3 [16]
Activation Energy (kJ/mol), E_d	90.3 [16]	

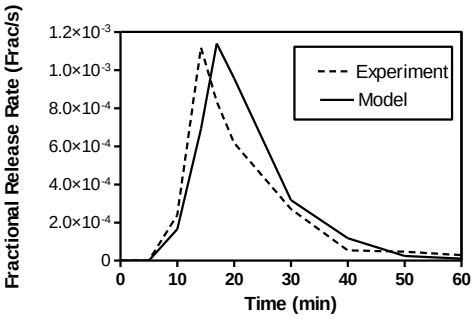

Fig. 4. Comparison between calculated and measured tritium fractional release rates (OSI-E23).

desorption at the grain surface, and diffusion through the network of interconnected pores.

A computer code has also been developed, based on the model. The code was used to calculate the tritium release in CREATE III and OSI-E23 out-of-pile experiments. The samples in both experiments were made of $LiAlO_2$. The case considered from the CREATE III experiment had a purge gas of He+1% H_2 and the other with a purge gas of pure helium. The case considered from the OSI-E23 experiment had a purge gas of Ar+0.1%H_2.

From the analysis of the model results and the comparisons with the experimental data, it was found that there is a good agreement between the CREATE III experiment and the model results, with a maximum error less than 15%. There is a time difference of about 3 min between the measured and calculated peaks in the OSI-E23 experiment. The calculated HT release was found to be faster than the measured release. The difference is attributed to assuming that there is no O_2 present in the system. There was less than 5% error between the calculated and measured fractional rate of tritium release.

References

[1] R.F. Mattas, and M.C. Billone, "Materials for Breeding Blankets", J. Nucl. Mater., 72-81, pp. 233-237 (1996).

[2] "Technical Basis for the ITER Final Design Report (FDR), Plant Description Documentation", IAEA/ITER EDA Documentation Series, Garching (2001).

[3] F. Elio, K. Ioki, P. Barabaschi, L. Bruno, A. Cardella, M. Hechler, T. Kodama, A. Lodato, D. Loesser, D. Lousteau, N. Miki, K. Mohri, R. Parker, R. Raffray, D. Williamson, M. Yamada, W. Daenner, R. Mattas, Y Strebkov, H. Takatsu, "Engineering Design of the ITER Blanket and Relevant R&D Results", Invited paper to the 20th SOFT, Marseille (7 -11 September (1998).

[4] A. Badawi, A.R. Raffray and M.A. Abdou, "Modeling and Analysis of Time-Dependent Tritium Transport in Lithium Oxide", J. Nucl. Mater., Vol. 273, pp. 79-94 (1999).

[5] A. Badawi, "Modeling and Analysis of Time-Dependent Tritium Transport in Lithium-Containing Ceramics", Ph.D. Dissertation, University of California at Los Angeles (1993).

[6] C.E. Johnson, K.R. Kummerer and E. Routh, "Ceramic Breeder Materials", J. Nucl. Mater., Vol. 155-157, pp. 188-201 (1988).

[7] G. Federici, A.R. Raffray and M.A. Abdou, "MISTRAL: A Comprehensive Model for Tritium Transport in Lithium-Base Ceramics- Part I: Theory and Description of Model Capabilities", J. Nucl. Mater., pp. 185-213, 173 (1990).

[8] M.C. Billone and R.G. Clemmer, "Modeling of Tritium Transport in Lithium Aluminate Fusion Solid Breeders," Fusion Technol., Vol. 8, pp. 875-880 (1985).

[9] A.Badawi, "Analysis of First and Second Order Surface Processes in Fusion Solid

Breeders", Alex. Eng. Journal, Vol. 39 (2), pp. 255 – 263 (2000).
[10] M.A. Pick and K. Sonnenberg, "A Model for Atomic Hydrogen-Metal Interactions – Applications to Recycling and Recombination", J. Nucl. Mater., Vol. 131, pp. 208-220 (1985).
[11] M. Boudart, H. Eyring, Physical Chemistry, Acadamic Press, New York (1975).
[12] A.K. Fischer and C.E. Johnson, Measurements of Adsorption in the $LiAlO_2$-H_2O System, Fusion Technology, Vol. 15, pp. 1212-1216 (1989).
[13] W.M. Jones, J. Chem. Phys., Vol. 17, pp. 1062-1064 (1949).
[14] A. Khaial, Analysis of Tritium Transport and Release in Out-of-Pile Experiments", M.Sc. Thesis, Alexandria University (2001).
[15] J.M. Miller, S.R. Bokwa and R.A. Verrall, "Post-Irradiation Tritium Recovery from Lithium Ceramic Breeder Materials", J. Nucle. Mater., Vol. 141-143, pp. 357-363 (1986).
[16] F. Botter, "Tritium Release Behavior from Lithium Aluminate Ceramics", Advances in Ceramics, Vol. 25, Eds. G.W. Hollenberg and I.J. Hastings, The American Ceramic Society, Ohio, pp. 61-72 (1989).
[17] H. Kudo, K. Okuno and S. O'Hira, "Tritium Release Behavior of Ceramic Breeder Candidates for Fusion Reactors", J. Nucl. Mater., Vol. 155-157, pp. 524-528 (1988).
[18] S. O'Hira, T. Hayashi, K. Okuno and H. Kudo, "Tritium Dissolution in and Release from Li2O", Fusion Eng. Des. Vol. 8, pp. 335-338 (1989).
[19] M. Glugla, K.H. Simon and R. D. Penzhorn, "The Solubility of Hydrogen in Lithium Metasilicate", J. Nucl. Mater., Vol. 155-157, pp. 513-515 (1988).

Received December 16, 2003
Accepted March 30, 2004